Sensors and Actuators A 152 (2009) 39–47

Contents lists available at ScienceDirect

Sensors and Actuators A: Physical

journal homepage: www.elsevier.com/locate/sna

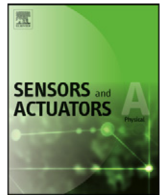

Stability of thin platinum films implemented in high-temperature microdevices

R.M. Tiggelaar [a], R.G.P. Sanders [b], A.W. Groenland [c], J.G.E. Gardeniers [a,*]

[a] *Mesoscale Chemical Systems, MESA+ Institute for Nanotechnology, University of Twente, P.O. Box 217, 7500 AE Enschede, The Netherlands*
[b] *Transducers Science and Technology, MESA+ Institute for Nanotechnology, University of Twente, P.O. Box 217, 7500 AE, Enschede, The Netherlands*
[c] *Semiconductor Components, MESA+ Institute for Nanotechnology, University of Twente, P.O. Box 217, 7500 AE, Enschede, The Netherlands*

ARTICLE INFO

Article history:
Received 19 December 2008
Received in revised form 19 March 2009
Accepted 20 March 2009
Available online 2 April 2009

Keywords:
Thin films
Microheaters
Platinum
Temperature sensors
Microreactors

ABSTRACT

In this paper we report on structural and electrical properties of thin films of Pt with Ti, Ta, or no adhesion, which were annealed in different ambient at temperatures in the range 400–950 °C. Correlations are made between the mechanical strain and grain size values obtained from X-ray diffraction, electrical measurements, and optical microscope images of film sintering after annealing at high temperature. A method to obtain highly adhesive, patterned Pt films without adhesion layer is presented, which films show the highest reliability, in terms of structural integrity and electrical properties. Therefore this is the best option for implementation in high-temperature microdevices like microreactors and gas sensors operating at temperatures above 750 °C.

© 2009 Elsevier B.V. All rights reserved.

1. Introduction

It has been reported frequently that thin film patterns of platinum (Pt), like temperature sensors or heaters, degrade at temperatures in the range 500–900 °C, which can lead to functional failure of the microdevices on which these patterns are deposited. We observed such a failure, for temperatures above ca. 700 °C, in our suspended-tube microreactors (see Fig. 5 of Ref. [1]). Other examples can be found in literature on microreactors [2,3] and micro-hotplate gas sensors [4–7], both categories of microdevices that operate at high temperatures, or ferroelectric memories and piezoelectric sensors and actuators where the active film is fired at high temperatures in an oxidizing ambient [8–10]. Typical evidence of progressing degradation is a change in the resistivity or in the temperature coefficient of resistance (TCR) [11–17], or roughening of the films and hillock or void formation [12,13,18–21]. Sometimes delamination of the film is observed, visible via blistering as the first stage of declining adhesion [11–13,18,20,22].

Thin films of noble metals like Pt do not adhere well to materials like silicon dioxide or silicon nitride. Therefore an intermediate layer between the Pt layer and the substrate is often used to improve adhesion. This adhesion layer in most cases consists of a metal that is less noble than Pt so that it is more prone to form a stable bond with the substrate. Furthermore, slight interface alloying during deposition under high vacuum conditions ensures a stable bond of the adhesion layer and Pt. Detailed studies on the adhesive strength of metals revealed that the optimal thickness of the adhesion layer is 10–20 nm [23]. Titanium (Ti) and tantalum (Ta) are commonly used adhesion layers for intermediate-to-high temperature applications [12,24]. However, these thin adhesion layers, by their nature of being less noble than Pt, often are the cause of failure of platinum thin film patterns when exposed to high temperatures. Intermediate-to-high temperature failure of adhesion layer–Pt film combinations can be attributed to undesired reactions of the adhesion material, like interdiffusion and alloying with the Pt film or oxidation [12–14,20,22]. To assess this problem, we performed a study on the thermal stability of platinum thin films with and without adhesion layer, with a focus on the properties that are relevant for application of the films in heaters and temperature sensors in integrated microreactors or gas sensors. The influence of annealing time, temperature and ambient on structural properties like crystallographic orientation, grain size, oxidation, alloy formation, surface roughness and film integrity will be given. Furthermore, the influence of these annealing parameters on mechanical properties like adhesion and film strain, and on electrical properties like the TCR and resistivity will be reported.

2. Experimental

2.1. Thin film deposition

The substrates used in this study were 3-in. and 100 mm (1 0 0)-oriented silicon wafers. Some substrates were steam oxidized at 1150 °C to achieve 0.4–0.6 μm thick SiO_2 films, others were coated

* Corresponding author.
E-mail address: j.g.e.gardeniers@utwente.nl (J.G.E. Gardeniers).

0924-4247/$ – see front matter © 2009 Elsevier B.V. All rights reserved.
doi:10.1016/j.sna.2009.03.017

Table 1
Sputtering conditions and rates for the different metals studied in this work.

Metal	System	Power, P (W)	Pressure, p (Pa)	Deposition rate, r (nm/s)
Ti	a	250	0.09 ± 0.01	0.08 ± 0.02
	b	200	0.5	0.11 ± 0.01
Ta	a	200	0.1	0.22 ± 0.03
	b	200	0.5	0.11 ± 0.02
Pt	a	100	0.09 ± 0.01	0.28 ± 0.05
	a	200	0.1	0.44 ± 0.02 [a]
	b	200	0.5	0.42 ± 0.02

[a] Rate increased to 0.7 nm/s for strongly eroded target.

with a low pressure chemical vapor deposition (LPCVD) process using SiH_2Cl_2 and NH_3 gas, resulting in 50 nm–1 μm thick low-stress silicon-rich (SiRN) or stoichiometric (Si_3N_4) silicon nitride layers. Prior to oxidation or deposition the wafers were cleaned in fuming and boiling aqueous nitric acid and an aqueous hydrofluoric acid solution.

On these substrates metal layers were deposited by DC magnetron sputtering. In cases where Pt was deposited on Ta or Ti, the two metal films were deposited subsequently without breaking the vacuum. Two home-built deposition systems were used: (a) a system with 2 sputter guns with 2-in. targets and a substrate holder with temperature control up to 450 °C. During room-temperature depositions the substrate holder was cooled continuously to 21 ± 4 °C. Via a rotary pump and a cryogenic pump base pressures below 2×10^{-5} Pa were reached; this system allows co-sputtering with two targets; (b) a system with 3 sputter guns and 2-in. targets and a substrate holder without cooling or temperature control. This system has a load lock, a rotary pump and a turbo-molecular pump for obtaining base pressures of $(3 \pm 1) \times 10^{-5}$ Pa. Both systems have rotating substrate holders. The distance between substrate and target is 15 cm in system (a) and 18 cm in system (b). During sputtering, film thickness was controlled via a quartz oscillator crystal and previously determined calibration factors. Before each deposition run native oxide layers were removed from the targets (99.999% purity) by sputtering for at least 2 min at a power of 200 W and 0.1 Pa Ar (99.999% purity) pressure. All sputter deposition runs were performed at room-temperature, unless explicitly stated otherwise. Table 1 shows parameters and rates for the actual deposition runs on both systems, and Table 2 summarizes the Pt film configurations.

While the adhesive strength of as-deposited Pt/Ti and Pt/Ta layers was good, the adhesion of Pt films was moderate after deposition and rather poor after annealing (see Section 3). To improve adhesion of these films on SiO_2 coated silicon, a procedure was used in which first Pt was sputtered at room-temperature in Ar/O_2 atmosphere, leading to the formation of a thin layer of Pt_xO_{1-x}, followed by Pt sputtering to the desired thickness in pure Ar [25–27]. Annealing in Ar at temperatures between 400 and 1300 °C removed the oxygen from the first layer and stabilized the entire Pt thin film [25]. After this, all films survived an adhesion test with Scotch-tape [25,28]. Silicon nitride-coated silicon was first exposed to an SF_6-O_2 plasma (6:1 gas ratio, pressure 40 mTorr, power 60 W) for 100–105 s, which removes contamination and roughens the surface, leading to improved adhesion [1]. However, since it was found that for a blanket Pt deposition on complete silicon nitride-coated surfaces the adhesion after annealing was poor, the as-deposited films were patterned by defining 50 μm wide lines in a photoresist layer spin-coated on the sputtered Pt film. The uncovered Pt was exposed to oxygen plasma (60 s, pressure 10 mTorr, power 60 W) resulting in an oxide-passivated Pt layer. This layer has a yellow-brown appearance, whereas unexposed Pt preserves its original metallic shine. The thickness of the oxide on the Pt film is 10–12 nm [29]. After resist stripping, the unexposed Pt was removed in a mixture of H_2O, HCl and HNO_3 (ratio 8:7:1, temperature 90 ± 1 °C, etching time 2 min), in which the etch rate of passivated Pt films is highly reduced [29], whereas unexposed Pt dissolves fast [30]. Thickness measurements showed that no etching of plasma-exposed Pt occurred and that unexposed Pt etched at a rate of more than 100 nm/min. The adhesion of the resulting Pt patterns after annealing was found to be good.

Table 2
Platinum thin film configurations.

Film configuration	Pt layer (nm)	Adhesion layer (nm)
Pt/Ti	360	50
	150	20
Pt/Ta	100	15
	200	15
Pt	220	–

All deposited metal layers were annealed at temperatures up to 950 °C for different time periods and temperature ramps in either a tube furnace with N_2 (H_2O content 2–3 ppm) or O_2 flows (purity 99.999%), or in a furnace with air flow. The thin film samples were quenched to room-temperature by pulling them out of the hot zone of the furnace as fast as possible.

2.2. Thin film characterization

The as-deposited and annealed thin films were studied by X-ray diffraction (XRD). All diffraction angles 2θ in this paper are related to the Cu $K\alpha_1$ wavelength of 0.154060 nm (the Cu Kβ line was removed from the source radiation with a Ni filter). The angle-dependent instrumental line broadening of the diffractometer was estimated from a linear fit of the full-width-at-half-maximum (FWHM) value of 6 different diffraction peaks from single-crystal Si substrates, which was found to follow the equation:

$$\mathrm{FWHM}_{\mathrm{instrumental}} = 0.04^\circ + 3.6 \times 10^{-4} \times 2\theta \quad (1)$$

for the 2θ range of 28° to 107°. FWHM values mentioned below were corrected (see [31]) for this instrumental broadening, assuming Gaussian diffraction profiles. In all XRD spectra, the Si{0 0 4} substrate peak was located at a 2θ value within 0.01° of the tabulated value (69.13°). For some samples so-called "rocking curves" were measured, by which we understand a measurement with the detector fixed at a certain diffraction angle 2θ, while the angle between the sample and the X-ray beam is varied over an angle Ω. This measurement is used to determine the distribution through the film of grains with crystallographic orientation at a fixed angle 2θ. From the corrected FWHM of the diffraction peaks in the $\theta - 2\theta$ scans the average grain size D was derived, using the Scherrer equation [31].

As will be shown in Section 3, the as-deposited films have d_{111} values larger than the value for bulk polycrystalline Pt, 0.2665 nm, which suggests that the Pt lattice in the film is stretched in the direction perpendicular to the film surface. A likely reason for this is compressive stress due to *peening* [32], by which the subsurface layers of a sputtered film are compressed due to extensive bombardment by reflected neutral atoms, an effect that is especially prominent at the relatively low sputtering pressures used in our study. The in-plane compressive stress σ leads to a perpendicular lattice distortion which can be expressed as

$$d_{111}^{\sigma} = d_{111}^{0}\left(1 - \frac{2\nu}{E}\sigma\right) \quad (2)$$

with ν is the Poisson ratio and E the elasticity modulus of Pt, and under the assumption that the films are very thin compared to the substrate. In-plane *compressive stress*, which by definition

has a negative value, thus leads to an out-of-plane *lattice expansion*. For a study of the exact mechanisms of lattice deformation more elaborate X-ray diffraction procedures should be followed [33], and alternatively, residual film stress can be determined also from wafer curvature [34]. This was however not our purpose, we merely would like to compare different films, annealed under different conditions, and will use the XRD data on the d_{111} lattice parameter only as an indication for a trend in average film strain, following the simple reasoning leading to Eq. (2), see also Ref. [35]. The effect of annealing, whatever the origin of the film strain is, will be that the material will restore a strain-free state by processes like self-diffusion, recrystallization and grain growth, which for long enough annealing intervals will lead to a completely relaxed film at the temperature of annealing. Experiments in which the annealing time was varied showed that less than 2 min of annealing at 700 °C is enough to completely relax the film, in which time also the grain size in the thickness direction of the Pt layer has reached its final value. After cooling down at a high rate (as is the case in our experiments), a strain will result that corresponds to the thermal expansion difference α between the film and the substrate, and approximately proportional to the difference between the temperature of annealing and room temperature. Assuming bulk values for α of $8.8 \times 10^{-6}\,K^{-1}$ for Pt, and $2.6 \times 10^{-6}\,K^{-1}$ for Si (both bulk values), the "thermal stress" in a Pt film on Si after cooling down from a high temperature will be tensile, which will lead to a contraction, and thus, according to Eq. (2), a lower d_{111} value.

Scanning electron microscopy (SEM) in a ISI system, equipped with a tracor energy-dispersive X-ray analysis (EDX) setup was used to study the composition of a number of films, and Auger electron spectroscopy (AES) was used to make compositional depth profiles of some films. Optical microscopy and atomic force microscopy (AFM) were used to study surface morphology, and the thickness and roughness of the films were measured with a step profiler. Electrical resistivity measurements were done with the aid of a Matheson four-point-probe station. Qualitative adhesion tests were done with the aid of conventional adhesive tape [28].

3. Results and discussion

In the following subsections the influence of the annealing time, temperature and ambient on structural properties (crystallographic orientation, grain size, oxidation, alloy formation, surface roughness and film integrity), mechanical (adhesion, strain) and electrical properties (TCR and resistivity) of Pt/Ti, Pt/Ta and Pt thin films will be shown. Unless mentioned otherwise, the results presented below are independent of the investigated composition of the Pt/Ti, Pt/Ta and Pt thin films, independent of whether the substrate was coated with silicon dioxide or silicon nitride, and independent of the applied sputter systems. In the last subsection the three Pt-based thin films will be compared, and implications for high-temperature applications of these films will be discussed.

3.1. Platinum/titanium thin films

Our results for the Pt thin films with Ti adhesion layer are very consistent with results from literature [18,36–43]. Both XRD and AES measurements showed evidence of oxidation of the Ti adhesion layer after annealing, which is enhanced in O_2-rich environments, where in the AES depth profiles it was also observed that Ti had diffused through the Pt film to form an oxide either embedded in or on top of the Pt film. SEM images revealed that Pt/Ti films annealed in O_2 were much rougher than samples annealed in N_2 (similar annealing temperatures and times), indicating the enhanced oxidation of Ti in O_2 environments.

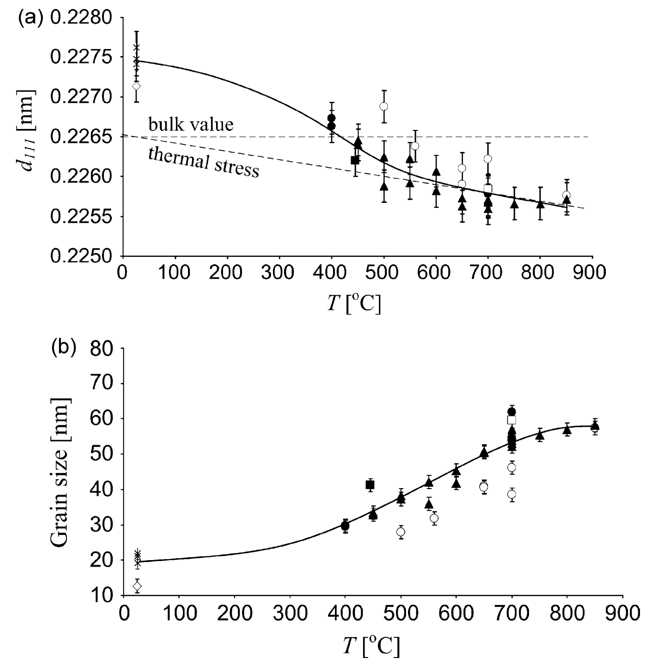

Fig. 1. XRD data for Pt with Ti adhesion layer (determined at room-temperature): (a) Pt{1 1 1} lattice spacing d_{111} and (b) grain size based on FWHM of Pt{1 1 1} diffraction peaks as a function of annealing temperature *T*. Symbols: (×) films deposited at 20 °C (non-annealed); (○) films annealed in N_2; (●) films annealed in O_2; (▲) films annealed in O_2 in consecutive runs; (■) films deposited at 445 °C (non-annealed); (□) films deposited at 445 °C and annealed in N_2; (◊) co-sputtered Pt_6Ti films. The solid line is a guide to the eye, not a model. See text for a definition of thermal stress.

In Fig. 1 the results of XRD-scans for a number of films before and after annealing at temperatures between 400 and 850 °C in N_2 and O_2 are summarized. Fig. 1(a) and (b) respectively show the Pt{1 1 1} spacing d_{111} and the grain size derived from the peak FWHM, both as a function of annealing temperature. The figures contain data for Pt/Ti films on SiO_2 and Si_3N_4, data for Pt/Ti deposited at 445 °C, as well as for a film co-sputtered from a Pt and a Ti target by adjusting the deposition rates of these elements in the ratio Pt:Ti = 6:1. A rocking curve measurement on Pt/Ti/SiO_2 samples gave FWHM values of ca. 6° for the {1 1 1} diffraction of as-deposited film as well as for films annealed at 700 °C, which indicates that the films are reasonably well-oriented along the ⟨1 1 1⟩ direction. Eq. (2) and the accompanying text (see Section 2.2) allows us to interpret the data in Fig. 1 as such that after annealing at increasingly higher temperatures, the d_{111} value decreases, approaches the dashed line which corresponds to the situation of thermal stress as explained in section 2.2, and runs along that line for temperatures above ca. 550 °C. The result for the film deposited at 445 °C is consistent with this proposal. The deposition temperature of 445 °C is above the Hüttig temperature, which is defined as 0.3 T_m with T_m the melting point in Kelvin. The Hüttig temperature roughly gives the onset of metal adatom mobility [44], which for Pt, with a melting point of 1768 °C, is 339 °C. It seems though that at the applied deposition rate, adatom mobility is still too low to completely compensate for the peening effect (assuming that peening is the cause for the d_{111} increase compared to bulk Pt).

In the XRD spectra of the Pt/Ti combination occasionally {2 0 0} diffractions were observed, for annealing at temperatures above 400 °C. For FCC metals like Pt, surface energy minimization favors grains with {1 1 1} texture, while strain-energy-minimization in films in which strain is elastically accommodated favors {2 0 0} texture [45]. It was argued that the {2 0 0} diffraction corresponds to crystallites (read: hillocks) grown on the Pt surface as a result of compressive strain relief [46], but our data do not support this,

because we never observed a {2 0 0} diffraction for other films than the Pt/Ti combination, while hillocks were observed on all films, after annealing. Most probably the {2 0 0} diffractions are not those of pure Pt, but of a compound Pt_3Ti [47].

Adhesion of the Pt/Ti films on siliconoxide or silicon nitride-coated silicon substrates in general was good for as-deposited and films annealed up to 550 °C in O_2 or N_2, but films annealed at higher temperatures showed decreasing adhesive quality, whereas annealing at 800 °C or higher led to a serious loss of adhesion, as evidenced by spherical delaminated regions.

The electrical resistivity of the Pt/Ti films was measured before and after annealing in N_2. For a 150 nm/20 nm Pt/Ti film the resistivity of the as-deposited film was 16 ± 2 μΩcm. After annealing for 10 min at 450 °C the resistivity increased to 21 ± 2 μΩcm, and kept increasing during prolonged annealing until after 100 min a steady-state value of 26 ± 2 μΩcm was reached (note that the resistivity of bulk Pt is 10.6 μΩcm). When a 360 nm/50 nm Pt/Ti film was annealed for 5 min at 700 °C, a resistivity of 53 ± 2 μΩcm was obtained. Longer annealing times at 700 °C resulted in increasing, irreproducible values for the resistivity. It is believed that this is caused by the formation of insulating TiO_x regions on the surface and in the bulk of the Pt layer. An increase in resistivity of annealed Pt/Ti films as a function of annealing settings was also observed by others; e.g. a resistivity of 34 μΩcm was found for ion-beam sputtered Pt/Ti films deposited at 200 °C and 90 μΩcm for films annealed at 500 °C, respectively [48]. For annealing temperatures above 700 °C, measured resistivity values of sputtered Pt/Ti films were found to increase dramatically. Particularly relevant in this respect is also the work of Schmid and co-workers [15–17], who have found that the resistivity of electron-beam-evaporated Pt/Ti films for annealing temperatures up to 450 °C, the film resistivity basically is as expected for conduction through a thin Pt film, but for annealing temperatures of 600 °C and above, the diffusion of titanium into the top layer gives an increase in film resistivity, while at such high temperatures the onset of "plastic deformation effects occurring in the top layer lead to an additional increase of the film resistivity via geometrical effects", arising from the formation of microholes [15,17]. The formation of such holes, and agglomeration of Pt/Ti films after prolonged annealing at temperatures above 700 °C is similar to what was observed for Pt/Ta and Pt, and will be discussed below.

3.2. Platinum/tantalum thin films

With $Pt/Ta/SiO_2$, $Pt/Ta/Si_3N_4$ and Ta/SiO_2 films the same experiments were performed as for the Pt/Ti film combinations. XRD-spectra revealed that after annealing in O_2, the Ta film has completely oxidized, but in contrast to the case of TiO_x discussed before, the formed Ta_2O_5 stays at its position, see Fig. 2, which shows AES depth profiles of a $Pt/Ta/Si_3N_4/Si$ layer before and after annealing in O_2 for 20 min at 700 °C. It can be seen that, although Ta oxidizes completely, because oxygen diffuses through the Pt film [49], Ta does not diffuse into the Pt film [24,50]. Similar results were found for $Pt/Ta/SiO_2/Si$, for which it was reported that Ta does not react with SiO_2 below 1000 °C [51]. According to the AES data, the Ta layer considerably increased in thickness after oxidation [52].

In Fig. 3 measured d_{111} and grain size values for Pt/Ta films are shown as a function of annealing temperature in N_2, O_2 and air. Pt/Ta films show similar trends as for the Pt/Ti films in Fig. 1, but differences in annealing ambient are less pronounced. Experiments as a function of annealing time for a temperature of 650 °C show that relaxation of compressive intrinsic stress requires only 30 s, which suggests that the underlying relaxation mechanism is a recrystallization process rather than a diffusion process. Furthermore, the grain size demonstrates the largest increase in the first minutes before reaching a steady-state value. Rocking curves on Pt/Ta films

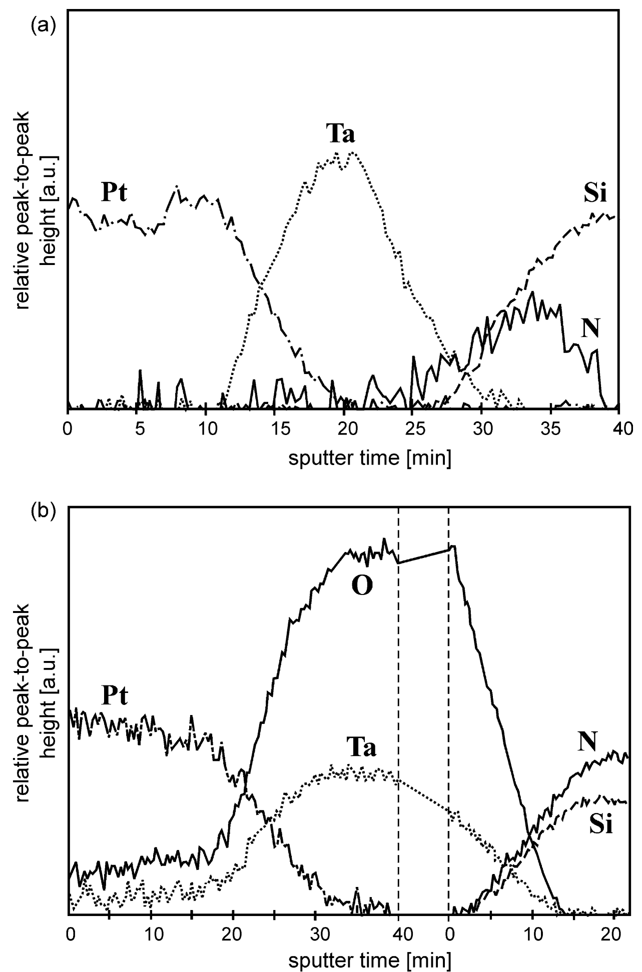

Fig. 2. AES depth profiles of $Pt/Ta/Si_3N_4$ package (200 nm Pt/50 nm Ta) before (a) and after (b) annealing for 20 min in O_2 at 700 °C.

show {1 1 1} texture for the Pt layer, with a FWHM varying from 2.4° to 5.6°. A slight decrease in the rocking curve FWHM of a few tenths of a degree was observed after annealing.

Pt/Ta films preserve their as-deposited smooth surfaces for annealing temperatures up to 550 °C, independent of the ambient. As can be seen in the photographs of Fig. 4, for annealing temperatures up to 750 °C hillocks are formed, which increase in number as well as in size, accompanied by a significant increase in surface roughness, as was determined by surface profile measurements. At 850 °C, the number of hillocks has decreased, and the hillocks start to flatten. Above 850 °C only a few flattened hillocks remain, and voids appear, which above 900 °C perforate the complete Pt/Ta film completely, finally resulting in the formation of separate metal islands. Similar effects were observed by Firebaugh et al. for both Pt/Ti and Pt/Ta films [12]. Fig. 4 shows that under the same conditions, a thinner film experiences faster and more severe agglomeration. Annealing with a slower temperature ramp (5 °C/min instead of 10 °C/min) enhances agglomeration, which was also reported in Ref. [12]. As a proof that the thermal budget is important rather than the highest temperature at which annealing occurs, we find that films pre-annealed first for 1 h at a temperature above 450 °C, and subsequently for 1 h at a higher temperature, contained more voids and islands than films annealed for 1 h at that high temperature only. Similar to what was reported by Firebaugh et al. [12], annealed Pt/Ta films showed a slight increase in thickness with increasing temperature, which may be interpreted as progressing agglomeration. The adhesion of the Pt/Ta films on

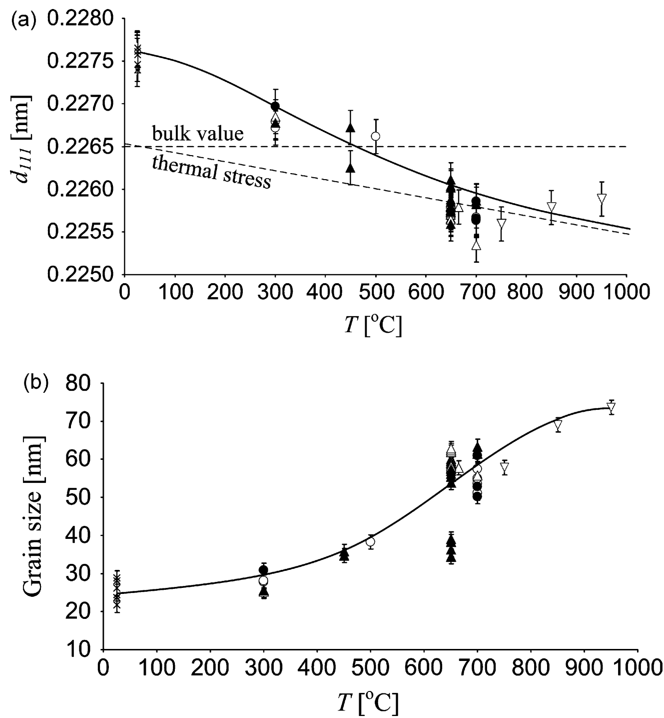

Fig. 3. XRD data for Pt with Ta adhesion layer (determined at room-temperature): (a) Pt{1 1 1} lattice spacing d_{111} and (b) grain size based on FWHM of Pt{1 1 1} diffraction peaks as a function of annealing temperature T. Symbols: (×) films deposited at 20 °C (non-annealed); (○) films annealed in N_2; (●) films annealed in O_2; (▽) films annealed in air; (△) films annealed in N_2 in consecutive runs; (▲) films annealed in O_2 in consecutive runs.

SiO_2 and Si_3N_4 was excellent for as-deposited films and remained very good for all Pt/Ta films subjected to annealing temperatures up to 950 °C, despite the agglomeration at elevated temperatures.

Four-point-probe measurements on as-deposited Pt/Ta films gave a resistivity of 19 ± 2 μΩcm, which did not change after annealing for 4.5 h in N_2 at 450 °C, which is in agreement with the data for Pt/Ta films annealed in air, see Table 3 (measurement performed in air; ramp-up 10 °C/min, kept for 1 h at indicated temperature; TCR and resistivity values were obtained from resistance–temperature calibration curves measured over the range 20–70 °C). The resistivity ρ decreases slightly for annealing up to 750 °C, above 750 °C the resistivity of 100 nm/15 nm Pt/Ta increased dramatically, due to severe agglomeration which led to a discontinuous film. For thicker Pt/Ta films (200 nm/15 nm) the resistivity stabilizes at a value of about 0.8 times the resistivity of as-deposited Pt/Ta films, indicating that this agglomerated film remains continuous. The TCR of annealed Pt/Ta films is almost constant up to 550 °C, above that temperature the TCR increases significantly. The final value (Table 3) is very close to the values reported for 800–1100 nm thick Pt films on alumina, annealed at 1250 and 1300 °C [53], but still significantly below the value of bulk Pt (3928.9 ppm K^{-1} [54]). Resistivity values were not influenced by slower temperature ramps nor by consecutive annealing steps, but due to increased agglomeration of Pt/Ta annealed with a slower ramp, the TCR of these films is higher than that of Pt/Ta films annealed with a ramp of 10 °C/min. However, for Pt/Ta films annealed in two consecutive steps as described above, TCR values were slightly lower than films annealed only at one temperature, an effect that was independent of the Pt thickness.

Due to progressing agglomeration the TCR and resistivity of Pt/Ta thin films operated at high temperatures display drift, which dictates frequent calibration if these films are used in heaters or temperature sensors. If the maximum operation temperature is below a ‘burn-in’ temperature $T_{burn-in}$ which is significantly higher than the operation temperature, the TCR and resistivity are stable for several tens of hours, due to film stress relaxation. If the film is subsequently operated at temperatures lower than $T_{burn-in}$, the overall degradation proceeds only very slowly. The length of the period that TCR and resistivity remain constant is influenced significantly by the composition of the thin film [1].

3.3. Platinum thin films

The lattice spacing values d_{111} and FWHM of the {1 1 1} peaks resulting from XRD measurements on Pt samples without adhesion layer, as-deposited and after different annealing steps, are shown in Fig. 5. The data show similar trends as the ones for Pt/Ti in Fig. 1 and for Pt/Ta in Fig. 3. No clear influence of annealing ambient (N_2, O_2

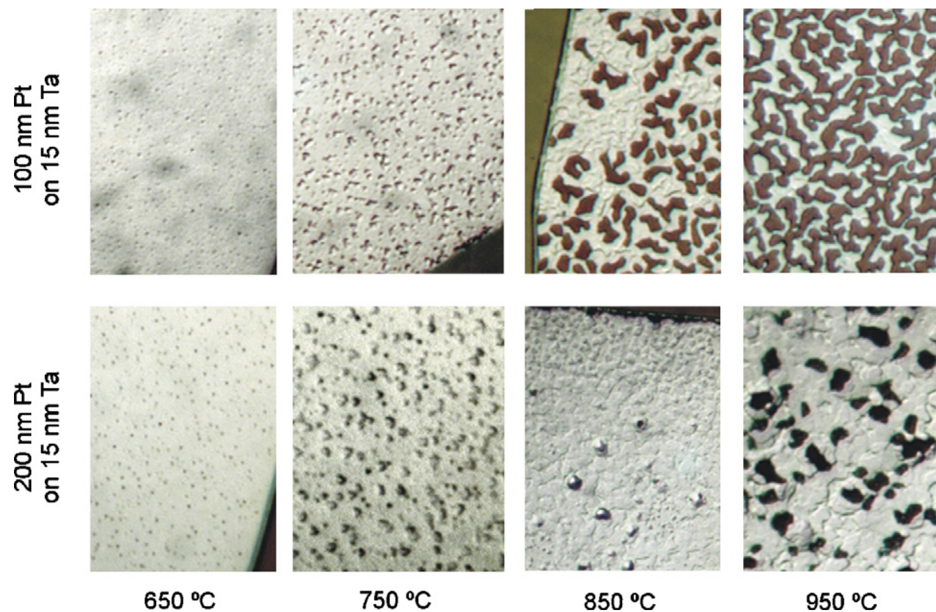

Fig. 4. Typical optical microscope pictures of Pt/Ta films annealed in air at different temperatures. For all samples the annealing conditions were: ramp up 10 °C/min and kept for 1 h at (indicated) temperature. Scales: 650 °C and 750 °C 500× magnification, 850 °C and 950 °C 1000× magnification.

Table 3
Electrical data of annealed Pt films with different adhesion layers.

Annealing temp. (°C)	100 nm Pt/15 nm Ta		200 nm Pt/15 nm Ta	
	ρ (μΩcm)	TCR (×10^{-3} °C^{-1})	ρ (μΩcm)	TCR (×10^{-3} °C^{-1})
250	19 ± 1	2.3 ± 0.1	16 ± 1	2.5 ± 0.1
450	21 ± 1	2.4 ± 0.1	18 ± 1	2.6 ± 0.1
550	21 ± 1	2.4 ± 0.1	18 ± 1	2.7 ± 0.1
650	19 ± 1	2.6 ± 0.1	18 ± 1	2.7 ± 0.1
750	17 ± 1	2.9 ± 0.1	15 ± 1	3.0 ± 0.1
850	∞	3.6 ± 0.1	14 ± 1	3.4 ± 0.1
950	∞	3.7 ± 0.1	15 ± 1	3.4 ± 0.1

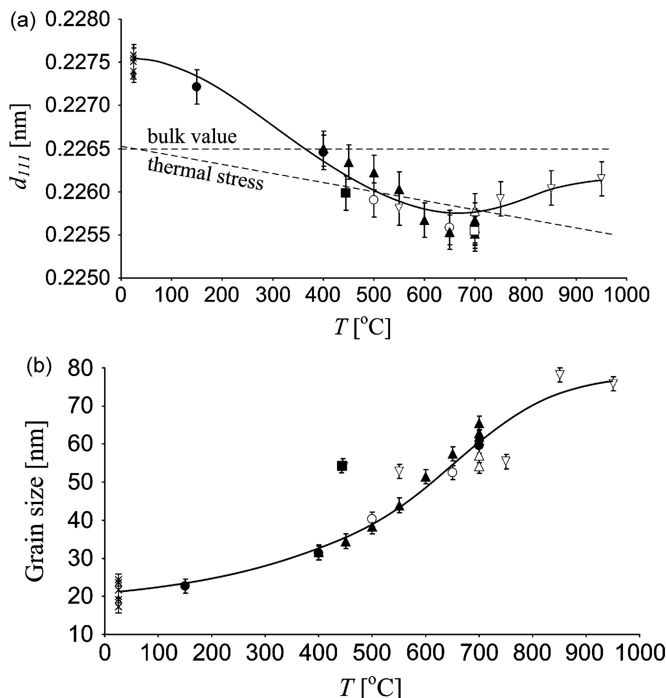

Fig. 5. XRD data for Pt without adhesion layer (determined at room-temperature): (a) Pt{1 1 1} lattice spacing d_{111} and (b) grain size based on FWHM of Pt{1 1 1} diffraction peaks as a function of annealing temperature T. Symbols: (×) films deposited at 20 °C (non-annealed); (○) films annealed in N_2; (●) films annealed in O_2; (▽) patterned films annealed in air; (△) films annealed in N_2 in consecutive runs; (▲) films annealed in O_2 in consecutive runs. (■) films deposited at 445 °C (non-annealed); (□) films deposited at 445 °C and annealed in N_2.

or air) is observed. Rocking curves on the (1 1 1) diffraction gave a FWHM value of 5.3° for an as-deposited and 4.4° for a layer annealed at 700 °C in N_2 (20 min). For a film deposited at 445 °C a much lower FWHM was found, just as for Pt/Ti deposited at this temperature. The in-plane strain in this film is tensile (in contrast to Pt films deposited at room-temperature which have compressive strain), but shifts to the general trend values after annealing. Rocking curve widths found for this film were 2.2° for as-deposited films and 1.8° for films annealed in N_2 at 700 °C for 20 min, which are substantially lower than the values found for the films deposited at room temperature.

As mentioned in Section 2, the adhesion of as-deposited Pt films on SiO_2 or Si_3N_4 is moderate, and becomes worse after annealing, especially for annealing above 500 °C, where blister formation and occasionally also delamination of parts of the films was observed. To improve adhesion without the use of an adhesion layer, a procedure was developed that effectively roughens the surface (see Section 2; the patterned films discussed below were sputtered on substrates that were treated with this procedure). Just like the Pt/Ta films, these Pt films keep their as-deposited smooth surfaces for annealing temperatures up to 550 °C, independent of ambient, while for higher temperatures hillocks and voids are observed, see Fig. 6. It was observed that for similar annealing conditions the size and height of the hillocks is much larger, terracing is more pronounced and starts, just like void formation, at a lower temperature for 220 nm Pt films, compared to 200 nm/15 nm Pt/Ta. Furthermore, with a slower ramp or with consecutive annealing steps more agglomeration is visible. Lee and Kim, in an AFM study on rapid thermal processing effects on very thin Pt films on SiO_2, found a distinct difference in behavior between films with a thickness in the range 3–15 nm compared to films of 30 nm and thicker [55]. The thinner films roughen after 1 min at 230 °C, while after 1 min at 300 °C dewetting via island formation occurs. For 30 nm films, no visible change occurred up to 600 °C, from that temperature on holes form and the films breaks up, until at ca. 800 °C the film becomes discontinuous. Our Pt films fall into the second category, and show very similar thermal behavior.

The electrical resistivity of as-deposited Pt films was 20 ± 2 μΩcm, which dropped after annealing at 450 °C in N_2 to 17 ± 2 μΩcm and then remained constant for at least 6 h annealing. These values are higher than the bulk value of 10.5 μΩcm at 20 °C [56], but in reasonable agreement with reported values for sputtered Pt films of 15–25 μΩcm [57]. In Table 4 the resistivity and TCR of Pt films annealed in air are listed (measurement details: ramp up 10 °C/min, kept for 1 h at indicated temperature). The TCR

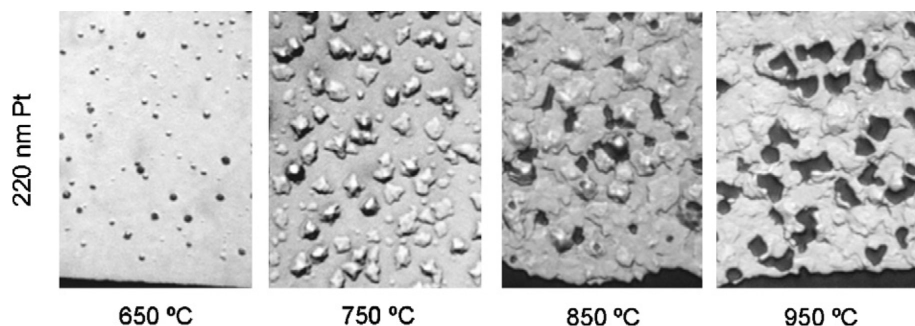

Fig. 6. Typical optical microscope pictures of patterned Pt films without adhesion layer annealed in air at different temperatures. For all samples the annealing conditions were: ramp up 10 °C/min and kept for 1 h at (indicated) temperature. Scales: 650 °C and 750 °C 500× magnification, 850 °C and 950 °C 1000× magnification.

Table 4
Electrical data of annealed 220 nm thick Pt films.

	Annealing temp. (°C)						
	250	450	550	650	750	850	950
ρ (μΩcm)	16 ± 1	14 ± 1	13 ± 1	13 ± 1	13 ± 1	13 ± 1	15 ± 1
TCR ($\times 10^{-3}$ °C^{-1})	2.3 ± 0.1	2.6 ± 0.1	2.8 ± 0.1	3.0 ± 0.1	3.2 ± 0.1	3.5 ± 0.1	3.6 ± 0.1

and resistivity values were obtained from resistance–temperature calibration curves measured over the range 20–70 °C after annealing. The resistivity is hardly influenced by annealing and stabilizes at about 80 ± 5% of the resistivity of the as-deposited film. The results are comparable to the 200 nm/15 nm Pt/Ta films. The TCR of pure Pt rises linearly with annealing temperature. The trends observed for resistivity and TCR of Pt films were not changed by slower temperature ramps nor by consecutive annealing steps. It can be concluded that the values for resistivity and TCR of Pt films are fixed by the highest temperature to which the film has been subjected, and that, although severe agglomeration is observed in these films, they stay coherent. The latter follows from the electrical measurements, which still gave reproducible values for the highest annealing temperature studied.

3.4. Comparison Pt/Ti, Pt/Ta and Pt thin films and implications for sensors and actuators

In comparison, the trends in the XRD results for all three film systems are very similar. The d_{111} value – which, as discussed above, is considered a measure for film residual stress – is higher than the bulk value for the as-deposited films, and with increasing annealing temperature approaches a value that corresponds with a film completely relaxed at the temperature of annealing but with a tensile stress after cooling to room temperature due to the thermal expansion difference between film and substrate. For annealing temperature above 700–800 °C the d_{111} value starts to deviate from the thermal stress value, and shows a tendency towards the bulk value. Within this temperature range also visible agglomeration sets in, at a somewhat lower temperature for the Pt films without adhesion layer than for the other films. Agglomeration and the tendency towards bulk Pt lattice values are related, in the sense that after agglomeration the disconnected crystallites will experience less of the mechanical constraints *set* by the substrate. Since this temperature range is above the Tammann temperature (defined as $0.5\,T_m$, with T_m the melting point in Kelvin [58]; for Pt the Tammann temperature is 748 °C), where bulk mobility is high, the Pt crystallites will re-flow during cooling down to ca. 700 °C, from which temperature on the material freezes and will follow the thermal stress value. Definite conclusions on the mechanism can only be obtained from XRD measurements in situ during high-temperature cycling. Such measurements have been performed by Nakamura et al. but unfortunately only until 600 °C [59]. The lattice change of 0.35% which they find after annealing of Pt/Ti (deposited at 200 °C) at 600 °C and cooling down to room temperature is in line with the value of 0.57% found in our study, Fig. 1(a).

The grain size values are in accordance with a mechanism of crystallite growth with increasing temperature, leading to significantly larger crystallites in the case of Pt/Ta and Pt without adhesion layer (ca. 70 nm) compared to Pt/Ti (ca. 55 nm). A reason for this may be that the TiO_2 precipitates present *in* and, more importantly, *on* the Pt/Ti layer after annealing inhibit Pt grain growth. Such a mechanism is absent in the other two film systems.

In this context it is also worth mentioning that the XRD data in Fig. 1 show a significant difference between annealing in N_2 and O_2. The films annealed in N_2 consistently show higher d_{111} and lower grain size values, except for the experiment at 850 °C, where the values are close to those obtained for O_2-annealed samples. This indicates that the processes of strain relief and grain growth are slower during N_2 annealing. This finding seems to be unrelated to Ti oxidation, because titanium oxide formation in the N_2-annealed samples clearly has occurred, as can be seen in Fig. 2, which oxidation is caused by the few ppm of H_2O present in the used N_2 gas. A likely explanation is that the enhanced strain relief and grain growth in O_2-annealed samples is caused by a mechanism in which Pt surface mobility is enhanced by oxygen. This is supported by the work of Rothschild et al. [60], who conclude from their experiments on Pt catalyst particles dispersed on alumina that two different modes of Pt coarsening (i.e., Pt grain growth) exist: (i) in hydrogen Pt sinters in an Ostwald ripening process through migration of Pt atoms, and (ii) in air or oxygen, PtO_2 is formed and vaporized (at very high temperature). Pt particles grow mainly by surface migration of PtO_2. Furthermore, their TEM experiments demonstrate that sintering in oxygen and air leads to significantly larger Pt particles (and at a considerably faster rate) than sintering in hydrogen. The difference in sintering rate begins to increase at temperatures above 500 °C. Similar results were found by Chen and Schmidt [61], who studied sintering of Pt crystallites on SiO_2 in air and N_2, and specifically mention that H_2O present in these gases inhibits particle growth. Thus, although the Pt is in a different form in these studies (Pt particles on a support) compared to our work (Pt grains in a homogeneous, supported thin film, at least at temperatures below ca. 800 °C), the similarities in grain growth behavior are very striking.

On the other hand, this mechanism of enhanced or inhibited Pt surface mobility seems not be active for Pt/Ta and Pt without adhesion layer, where no obvious difference can be seen between annealing in N_2 or O_2. Possibly a combination of the presence of TiO_2 precipitates (which above was concluded to inhibit grain growth) and the ambient effect on Pt surface mobility play a role in the case of the Pt/Ti films.

With respect to agglomeration, since the annealing temperatures studied in our work are close to or above the Tammann temperature of Pt, we conclude from our observations that the mobility of Pt nanocrystallites is higher on SiO_2 and Si_3N_4 than on Ta_2O_5. Similar observations were made for dispersed Pt catalyst on SiO_2 [61] and Al_2O_3 [62], which is quite comparable to Ta_2O_5 in terms of wettability. We were not able to find wetting properties for Pt on the respective surfaces, but data for water contact angles can be used as an indication. These angles are ca. 60° for Ta_2O_5 and 80° for TiO_2 [63], 65° for Al_2O_3 [64] and ca. 40° for (dehydroxylated) SiO_2 [65], which indicates that the water wettability (hydrophilicity) increases in the range $TiO_2 < Al_2O_3$, $Ta_2O_5 < SiO_2$. Since Si_3N_4 will have a very thin oxide layer, this material will be very close to SiO_2 in surface energy. Taking into account that it has been reported that Al_2O_3 as adhesion layer increases the stability of Pt films up to temperatures of 1000 °C [66], which we consider proof of the good wettability of alumina by Pt, the hydrophilicity order obviously is the reverse order in which Pt wets these surfaces, or put differently, Pt will agglomerate more if the surface is more hydrophilic, provided that adatom and nanoparticle mobility is high enough. This order is consistent with our observations of agglomeration.

Depending on the specific application of the Pt films, and the temperature window in which the application is expected to operate stably and reliably, a choice may be made on a specific combination of Pt film and adhesion layer. In Table 5 a summary of the

Table 5
Summary of Pt/Ti, Pt/Ta, and Pt thin film properties after high-temperature annealing.

Aspect/material	Pt/Ti thin films	Pt/Ta thin films	Pt thin films
Adhesion layer diffusion	Yes	No	No
Adhesion layer reaction	TiO_x, in and near Pt–substrate interface	Ta_2O_5, near Pt–substrate interface	No
Agglomeration of Pt	Yes	Yes	Yes
Adhesion of thin film	Good < 450 °C, poor > 550 °C	Excellent	Good (special procedure)
Electrical behavior	Reliable < 650 °C	Reliable < 850 °C	Reliable > 850 °C

properties studied in this paper and the corresponding results is given. This table may serve as a guide for the selection of a film for a specific microdevice. For applications below 450 °C Pt/Ti can be used without major problems. For temperatures above 550 °C the adhesion of Pt/Ti films fails, electrical problems start to occur above 600 °C. For applications in which the temperature of Pt-based thin films may exceed 450 °C the use of Pt/Ta or Pt is prefered, in this temperature range the electrical properties and adhesion of these thin films are significantly better than those of Pt/Ti. The electrical properties of both Pt/Ta and Pt are nearly independent of the annealing conditions up to 850 °C, but the long term electrical behavior of Pt is superior to Pt/Ta. Whereas Pt/Ta exhibits an excellent adhesion for annealing temperatures up to 950 °C, a special deposition and patterning procedure is required to have good adhesion of Pt after annealing. It is noteworthy that exposure to temperatures above 800 °C for long periods (h), all Pt films will eventually agglomerate or sinter. For a thin film sensor or heater this is detrimental, because it leads to spatial differences in the thickness of the film, in its turn leading to local electrical resistance changes and therewith changes in sensor or heater characteristics. In the end this may lead to disruption or burn-out of the electronic circuit in which the sensor or heater is embedded, which was observed in our earlier work [1] and in work of others [5,6]. By selecting proper annealing parameters and thin film compositions these degradation effects can be slowed down, such that Pt-based thin films can be used reliably for a significantly long period at high temperatures, but failure cannot be prevented.

4. Summary and conclusions

In this work structural, electrical and mechanical aspects of thin films of Pt/Ti, Pt/Ta and Pt without an adhesion layer annealed at temperatures in the range 400–950 °C (in N_2, O_2 and air) were investigated. XRD data showed that films as-deposited have a compressive in-plane stress and an average grain size of ca. 20 nm. After annealing, and independent of the type of film, stress is relaxed via a process of grain growth and hillock formation, leading to a Pt lattice parameter which approaches the value arising from the thermal expansion difference between the Pt and the silicon substrate, and after annealing at temperatures above ca. 700 °C, where hole formation and film agglomeration is observed, to a lattice parameter close to that of bulk Pt. Pt/Ti films showed a different annealing behavior than the Pt/Ta and Pt films, with a clear effect of annealing ambient, where nitrogen annealing leads to slower grain growth and slower stress relaxation (the latter being a result of the first), in which possibly also the formation of TiO_x precipitates in or on the Pt film played a role.

Due to continuous structural degradation above 500 °C the resistivity and the temperature coefficient of resistance exhibit drift, resulting in a restricted lifetime for reliable operation at elevated temperatures, especially for Pt/Ti thin films, due to diffusion of Ti into the Pt layer, severe oxidation of Ti and agglomeration of the Pt layer. Above 650 °C the electrical properties and adhesion of Pt/Ta thin films are significantly better than those of Pt/Ti films. The resistivity and TCR of Pt/Ta and Pt without adhesion layer hardly depends on annealing temperature up to 850 °C. Experiments revealed that after 'burn-in' Pt showed a better long-term electrical behavior than Pt/Ta with identical thickness. However, Pt adhesion had to be improved, which was done by roughening the Si_3N_4 surface on which the Pt should adhere, and patterning the Pt in order to reduce stresses acting during annealing steps.

All the above-mentioned aspects should be taken into account when platinum-based thin films are to be used as reliable and stable thin film heaters and temperature sensors in high-temperature microdevices.

Acknowledgements

The authors thank Johnny Sanderink for sputtering depositions, Bert Otter for SEM and AFM measurements, Albert van den Berg for AES measurements, Poul de Haan for countless discussions on XRD, Albert Prak for electrical data, and Kees Eijkel and the members of the Transducers Science and Technology Group at the MESA+ Institute for Nanotechnology for stimulating discussions. This research was partially supported by the Technology Foundation STW, applied science division of NWO and the technology program of the Ministry of Economic Affairs of the Netherlands.

References

[1] R.M. Tiggelaar, J.W. Berenschot, J.H. de Boer, R.G.P. Sanders, J.G.E. Gardeniers, R.E. Oosterbroek, A. van den Berg, M.C. Elwenspoek, Fabrication and characterization of high-temperature microreactors with thin film heater and sensor patterns in silicon nitride tubes, Lab Chip 5 (2005) 326–336.
[2] C. Alépée, L. Vulpescu, P. Cousseau, P. Renaud, R. Maurer, A. Renken, Microsystem for high-temperature gas phase reactions, Meas. Control 33 (2000) 265–268.
[3] L.R. Arana, S.B. Schaevitz, A.J. Franz, M.A. Schmidt, K.F. Jensen, A microfabricated suspended-tube chemical reactor for thermally efficient fuel processing, J. Microelectromech. Syst. 12 (2003) 600–612.
[4] S.V. Patel, M. DiBattista, J.L. Gland, J.W. Schwank, Survivability of a silicon-based microelectronic gas-detector structure for high-temperature flow applications, Sens. Actuators B 37 (1996) 27–35.
[5] D. Briand, F. Beaudoin, J. Courbat, N.F. de Rooij, R. Desplats, P. Perdu, Failure analysis of micro-heating elements suspended on thin membranes, Microelectron. Reliab. 45 (2005) 1786–1789.
[6] J. Courbat, D. Briand, N.F. de Rooij, Reliability improvement of suspended platinum-based micro-heating elements, Sens. Actuators A 142 (2008) 284–291.
[7] H. Esch, G. Huyberechts, R. Mertens, G. Maes, J. Manca, W. De Ceuninck, L. De Schepper, The stability of Pt heater and temperature sensing elements for silicon integrated tin oxide gas sensors, Sens. Actuators B 65 (2000) 190–192.
[8] A. Grill, W. Kane, J. Viggiano, M. Brady, R. Laibowitz, Base electrodes for high dielectric constant oxide materials in silicon technology, J. Mater. Res. 7 (1992) 3260–3265.
[9] G.A.C.M. Spierings, G.J.M. Dormans, W.G.J. Moors, M.J.E. Ulenaers, P.K. Larsen, Stresses in $Pt/Pt(Zr,Ti)O_3/Pt$ thin-film stacks for integrated ferroelectric capacitors, J. Appl. Phys. 78 (1995) 1926–1933.
[10] K. Numata, K. Aoki, Y. Fukuda, A. Nishimura, Annealing effects to electrode Pt/Ti for PZT, Mater. Res. Soc. Symp. Proc. 318 (1993) 659–665.
[11] R. Srinivasan, I.-M. Hsing, P.E. Berger, S.L. Firebaugh, M.A. Schmidt, M.P. Harold, J.J. Lerou, J.F. Ryley, Micromachined reactors for catalytic partial oxidation reactions, AIChE J. 43 (1997) 3059–3069.
[12] S.L. Firebaugh, K.F. Jensen, M.A. Schmidt, Investigation of high-temperature degradation of platinum thin films with an in situ resistance measurement apparatus, J. Microelectromech. Syst. 7 (1998) 128–135.
[13] C. Alépée, Technologies for high-temperature silicon microreactors, Ph.D. thesis, École polytechnique fédérale de Lausanne (EPFL), Lausanne, Switzerland, 2000.
[14] J.-S. Lee, H.-D. Park, S.-M. Shin, J.-W. Park, Agglomeration phenomena of high temperature coefficient of resistance platinum films deposited by electron beam evaporation, J. Mater. Sci. Lett. 16 (1997) 1257–1259.
[15] U. Schmid, The impact of thermal annealing and adhesion film thickness on the resistivity and the agglomeration behavior of titanium/platinum thin films, J. Appl. Phys. 103 (2008), nr. 054902.

[16] U. Schmid, H. Seidel, Effect of high temperature annealing on the electrical performance of titanium/platinum thin films, Thin Solid Films 516 (2008) 898–906.
[17] U. Schmid, H. Seidel, Influence of thermal annealing on the resistivity of titanium/platinum thin films, J. Vac. Sci. Technol. A 24 (2006) 2139–2146.
[18] E.A. Kneer, D.P. Birnie III, G. Teowee, J.C. Podlesny, Evolution of surface relief during firing of PZT thin films, Integr. Ferroelectr. 152 (1994) 67–73.
[19] P.D. Hren, H. Al-Shareef, S.H. Rou, A.I. Kingon, P. Buaud, E.A. Irene, Hillock formation in platinum films, Mater. Res. Soc. Symp. Proc. 260 (1992) 575–580.
[20] D. Briand, S. Heimgartner, M. Leboeuf, M. Dadras, N.F. de Rooij, Processing influence on the reliability of platinum thin films for MEMS applications, Mater. Res. Soc. Symp. Proc.; vol. 729, BioMEMS and Bionanotechnology, San Francisco, CA, USA, 2002 April, pp. 63–68.
[21] H.-J. Nam, D.-K. Choi, W.-J. Lee, Formation of hillocks in Pt/Ti electrodes and their effects on short phenomena of PZT films deposited by reactive sputtering, Thin Solid Films 371 (2000) 264–271.
[22] M.P. Moret, M.A.C. Devillers, F.D. Tichelaar, E. Aret, P.R. Hageman, P.K. Larsen, Damage after annealing and aging at room temperature of platinized silicon substrates, Thin Solid Films 434 (2003) 283–295.
[23] L.I. Maissel, R. Glang, Handbook of Thin Film Technology, McGraw-Hill, New York, USA, 1970.
[24] T. Maeder, L. Sagalowicz, P. Muralt, Stabilized platinum electrodes for ferroelectric film deposition using Ti, Ta and Zr adhesion layers, Jpn. J. Appl. Phys. 37 (1998) 2007–2012.
[25] D.S. Lee, D.I. Chun, D.Y. Park, J.W. Ha, E.J. Yoon, M.H. Kim, H.J. Woo, Method for deposting a platinum layer on a silicon wafer, United States Patent 5,736,422 (1998).
[26] H.J. Woo, D.Y. Park, D.S. Lee, D.I. Chun, E.J. Yoon, Apparatus and methods of depositing a platinum film with anti-oxidizing function over a substrate, United States Patent 6,054,331 (2000).
[27] R.C. Budhani, S. Prakash, H.J. Doerr, R.F. Bunshah, Summary abstract: oxygen enhanced adhesion of platinum films deposited on thermally grown alumina surfaces, J. Vac. Sci. Technol. A 4 (1986) 3023–3024.
[28] J. Strong, On the cleaning of surfaces, Rev. Sci. Instrum. 6 (1935) 97–98.
[29] M.J. Kim, L.A. Gruenke, R.J. Saia, S.S. Cohen, Inhibition of acid etching of Pt by pre-exposure to oxygen plasma, Appl. Phys. Lett. 33 (1984) 462–464.
[30] J.L. Vossen, W. Kern, Thin Film Processes, Academic Press, London, UK, 1978.
[31] H.P. Klug, L.E. Alexander, X-ray Diffraction Procedures for Polycrystalline and Amorphous Materials, 2nd edition, John Wiley and Sons, New York, USA, 1974.
[32] J.A. Thornton, D.W. Hoffman, Internal stresses in titanium, nickel, molybdenum, and tantalum films deposited by cylindrical magnetron sputtering, J. Vac. Sci. Technol. 14 (1977) 164–168.
[33] S.G. Malhotra, Z.U. Rek, S.M. Yalisove, J.C. Bilello, Analysis of thin film stress measurement techniques, Thin Solid Films 301 (1997) 45–54.
[34] G.G. Stoney, The tension of metallic films deposited by electrolysis, Proc. R. Soc. London A 82 (1909) 172–175.
[35] R.W. Hoffman, The mechanical properties of thin condensed films, in: G. Hass, R.E. Thun (Eds.), Physics of Thin Films, vol. 3, Academic Press, New York, 1996, pp. 211–272.
[36] J.O. Olowolafe, R.E. Jones, A.C. Campbell, R.I. Hegde, C.J. Mogab, Effects of anneal ambients and Pt thickness on Pt/Ti and Pt/Ti/TiN interfacial reactions, J. Appl. Phys. 73 (1993) 1764–1772.
[37] K. Sreenivas, I. Reaney, T. Maeder, N. Setter, C. Jagadish, R.G. Elliman, Investigation of Pt/Ti bilayer metallization on silicon for ferroelectric thin film integration, J. Appl. Phys. 75 (1994) 232–239.
[38] U. Scheithauer, W. Hösler, R. Bruchhaus, Combined AES/factor analysis and RBS investigation of a thermally treated Pt/Ti metallisation on SiO_2, Fresenius J. Anal. Chem. 346 (1993) 305–307.
[39] G.R. Fox, S. Trolier-McKinstry, S.B. Krupanidhi, L.M. Casas, Pt/Ti/SiO_2/Si substrates, J. Mater. Res. 10 (1995) 1508–1515.
[40] A.E. Morgan, E.K. Broadbent, K.N. Ritz, D.K. Sadana, B.J. Burrow, Interactions of thin Ti films with Si, SiO_2, Si_3N_4, and SiO_xN_y under rapid thermal annealing, J. Appl. Phys. 64 (1988) 344–353.
[41] P.C. McIntyre, S.R. Summerfelt, Kinetics and mechanisms of TiN oxidation beneath Pt thin films, J. Appl. Phys. 82 (1997) 4577–4585.
[42] T.C. Tisone, J. Drobek, Diffusion in thin film Ti–Au, Ti–Pd, and Ti–Pt couples, J. Vac. Sci. Technol. 9 (1972) 271–275.
[43] R. Bruchhaus, D. Pitzer, O. Eibl, U. Scheithauer, W. Hösler, Investigation of Pt bottom electrodes for 'in-situ' deposited Pb(Zr, Ti)O_3 (PZT) thin films, Mater. Res. Soc. Symp. Proc. 243 (1992) 123–128.
[44] G.F. Hüttig, Catalytic activity and composition of oxide systems, Disc. Faraday Soc. 8 (1950) 215–222.
[45] C.V. Thompson, Structure evolution during processing of polycrystalline films, Ann. Rev. Mater. Sci. 30 (2000) 159–190.
[46] W.W. Jung, S.K. Choi, S.Y. Kweon, S.J. Yeom, Platinum(1 0 0) hillock growth in a Pt/Ti electrode stack for ferroelectric random access memory, Appl. Phys. Lett. 83 (2003) 2160–2162.
[47] A. Ehrlich, U. Weiß, W. Hoyer, T. Geßner, Microstructural changes of Pt/Ti bilayer during annealing in different atmospheres—an XRD study, Thin Solid Films 300 (1997) 122–130.
[48] H.N. Al-Shareef, K.D. Gifford, S.H. Rou, P.D. Hren, O. Auciello, A.I. Kingon, Electrodes for ferroelectric thin films, Integr. Ferroelectr. 3 (1993) 321–332.
[49] S.-K. Ko, N.M. Devashrajee, S.P. Murarka, Reactions of titanium films with thin silicon dioxide, nitride, and oxynitride films during rapid thermal annealing, Mater. Res. Soc. Symp. Proc. 260 (1992) 665–670.
[50] J.G.E. Gardeniers, R.W. Tjerkstra, A. van den Berg, Fabrication and application of silicon-based microchannels, in: Tech. Digest, 3rd International Conference on Microreaction Technology (IMRET 3), April 18–21, 1999, Frankfurt am Main, Germany, 1999, pp. 36–44.
[51] S.W. Russell, J.W. Strane, J.W. Mayer, S.Q. Wang, Reaction kinetics in the Ti/SiO_2 system and Ti thickness dependence on reaction rate, J. Appl. Phys. 76 (1994) 257–263.
[52] C. Cabral Jr., L.A. Clevenger, R.G. Schad, Compressive stress increase with repeated thermal cycling in tantalum(oxygen) thin films, Mater. Res. Soc. Symp. Proc. 308 (1993) 57–62.
[53] J. Zhang, Y. Nagao, S. Kuwano, Y. Ito, Microstructure and temperature coefficient of resistance of platinum films, Jpn. J. Appl. Phys. 36 (1997) 834–839.
[54] D.J. Curtmis, Temperature, Its Measurement and Control in Science and Industry, vol. 5, Instrument Society of America, Pittsburgh, PA, 1995, p. 803.
[55] J.-M. Lee, B.-I. Kim, Thermal dewetting of Pt thin film: etch-masks for the fabrication of semiconductor nanostructures, Mater. Sci. Eng. A 449 (2007) 769–773.
[56] D.R. Lide, Handbook of Chemistry and Physics, 77th edition, CRC Press Inc., New York, USA, 1996.
[57] B. Window, F. Sharples, N. Savvides, Plastic flow in ion-assisted deposition of refractory metals, J. Vac. Sci. Technol. A 6 (1988) 2333–2340.
[58] G. Tammann, Q.A. Mansuri, Metallographische Mitteilungen aus dem Institut für physikalische Chemie der Universität Göttingen CXIII. Zur Rekristallisation von Metallen und Salzen, Z. Anorg. Allg. Chem. 126 (1923) 119–128.
[59] K. Nakamura, Y. Otani, M. Kurita, S. Okamura, T. Shiosaki, Variation in 111 d-space and generation of hillocks in platinum thin-film electrodes by heat treatment, Jpn. J. Appl. Phys. 44 (2005) 8096–8101.
[60] W.G. Rothschild, H.C. Yao, H.K. Plummer Jr., Surface interaction in the Pt/γ-$A1_2O_3$ system. 5. Effects of atmosphere and fractal topology on the sintering of Pt, Langmuir 2 (1986) 588–593.
[61] M. Chen, L.D. Schmidt, Morphology and sintering of Pt crystallites on amorphous SiO_2, J. Catal. 55 (1978) 348–360.
[62] Y.F. Chu, E. Ruckenstein, On the sintering of platinum on alumina model catalyst, J. Catal. 55 (1978) 281–298.
[63] V. Rico, C. López, A. Borrás, J.P. Espinós, A.R. González-Elipe, Effect of visible light on the water contact angles on illuminated oxide semiconductors other than TiO_2, Sol. Energy Mater. Sol. Cells 90 (2006) 2944–2949.
[64] V. Anita, N. Saito, O. Takai, Microarc plasma treatment of titanium and aluminum surfaces in electrolytes, Thin Solid Films 506–507 (2006) 364–368.
[65] A. Kanta, R. Sedev, J. Ralston, Thermally- and photoinduced changes in the water wettability of low-surface-area silica and titania, Langmuir 21 (2005) 2400–2407.
[66] S. Halder, T. Schneller, R. Waser, Enhanced stability of platinized silicon substrates using an unconventional adhesion layer deposited by CSD for high temperature dielectric thin film deposition, Appl. Phys. A 87 (2007) 705–708.

Biographies

R.M. (Roald) Tiggelaar was born in Groningen (the Netherlands) in 1976. He received his MSc degree in Electrical Engineering in July 2000. From October 2000 to December 2004 he worked towards his PhD degree on the same university, on silicon-technology based microreactors for heteregenous catalytic partial oxidation reactions. Since January 2005 he works a post-doctoral researcher: on the development of glass microreactors for high-pressure organic chemistry, on glass-based microfluidic systems for highly efficient electrochemical cleavage of proteins, and currently on silicon-based microreactors for investigations on three-phase (gas–liquid–solid) catalytic reactions. His research interests focus on micro-electromechanical fabrication technologies, and silicon/glass microreactors and their applications.

R.G.P. (Remco) Sanders was born in Aarlanderveen (the Netherlands) in 1974. He received a bachelor degree in applied physics in December 1996 (Technische hogeschool Rijswijk). Since March 1997 he is working on the University Twente in the Transducer Science and Technology group as a technician. His main focus is design and fabrication of measurement techniques and setups for a wide range of micro-electromechanical devices.

A.W. (Alfons) Groenland was born in Hengelo (the Netherlands) in 1982. He received his BSc and MSc (cum laude) from the University of Twente, Enschede, the Netherlands, in 2005 and 2006, respectively. He is currently working towards his PhD degree in the Semiconductor Components Group, MESA+ Institute for Nanotechnology, University of Twente. His research topic is nanoscale sensors and actuators for chemical microreactor applications, with the focus on device fabrication and characterization.

J.G.E. (Han) Gardeniers (BSc: 1982; MSc: 1985; PhD: 1990) joined the Department of Electrical Engineering at the University of Twente, The Netherlands, as an assistant professor in 1990. From 2001 till 2003 he was employed as project leader MOEMS at Kymata Netherlands B.V./Alcatel Optronics Netherlands B.V. and as research manager at Micronit Microfluidics B.V., where he was responsible for R&D related to miniaturized chemical synthesis and analysis systems. In 2003 he rejoined the University of Twente, as an associate professor with the Biosensors/Lab-on-a-Chip Group. Since January 2007 he holds a personal chair in the field of Mesoscale Chemical Systems with the Science and Technology (TNW) Dept. of the University of Twente. He has published over 120 reviewed journal papers on various topics in materials science, microfabrication and microfluidics.